

# Rayleigh Scattering in Spectral Series with $L$ -Term Interference

R. Casini<sup>a</sup>, R. Manso Sainz<sup>b</sup>, and T. del Pino Alemán<sup>a</sup>

<sup>a</sup>*High Altitude Observatory, National Center for Atmospheric Research,<sup>1</sup>  
P.O. Box 3000, Boulder, CO 80307-3000, U.S.A.*

<sup>b</sup>*Max-Planck-Institut für Sonnensystemforschung,  
Justus-von-Liebig-Weg 3, 37077 Göttingen, Germany*

## ABSTRACT

We derive a formalism to describe the scattering of polarized radiation over the full spectral range encompassed by atomic transitions belonging to the same spectral series (e.g., the H I Lyman and Balmer series, the UV multiplets of Fe I and Fe II). This allows us to study the role of radiation-induced coherence among the upper terms of the spectral series, and its contribution to Rayleigh scattering and the polarization of the solar continuum. We rely on previous theoretical results for the emissivity of a three-term atom of the  $\Lambda$ -type taking into account partially coherent scattering, and generalize its expression in order to describe a “multiple  $\Lambda$ ” atomic system underlying the formation of a spectral series. Our study shows that important polarization effects must be expected because of the combined action of partial frequency redistribution and radiation-induced coherence among the terms of the series. In particular, our model predicts the correct asymptotic limit of 100% polarization in the far wings of a *complete* (i.e.,  $\Delta L = 0, \pm 1$ ) group of transitions, which must be expected on the basis of the principle of spectroscopic stability.

## 1. Introduction

The observation and analysis of the polarization signatures of resonant transitions in the solar spectrum have proven to be extremely useful for developing diagnostic tools of the magnetism of the top layers of the solar atmosphere (upper photosphere, chromosphere, transition region; see, e.g., the reviews by Stenflo 2015; Trujillo Bueno, Landi Degl’Innocenti, & Belluzzi 2017). Relatively recent discoveries that have been fostered by adding polarization information to the spectroscopic analysis of the solar radiation—such as the so-called “second solar spectrum” (Ivanov 1991; Stenflo & Keller 1997)—have revealed the potential of these diagnostics. Often, the observed polarization patterns have defied our ability to adequately model them, at times giving rise to “enigmas” about how the magnetism of the solar atmosphere is realized, and even to the point of questioning the very foundations of our theoretical understanding of polarized line formation (Stenflo 2011).

The modeling of the scattering polarization in the solar spectrum becomes particularly challenging in the UV, because of the high density of spectral features observed there. On the other

---

<sup>1</sup>The National Center for Atmospheric Research is sponsored by the National Science Foundation.

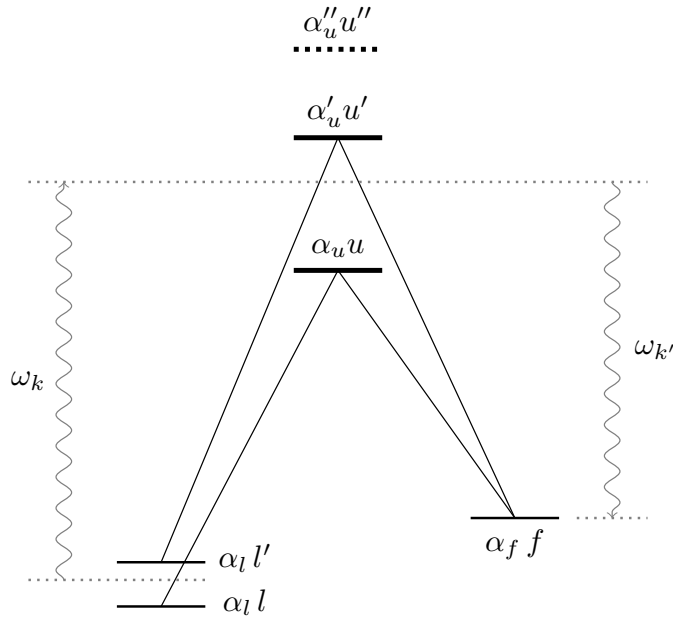


Fig. 1.— The “multiple  $\Lambda$ ” atomic model, with lower terms  $\alpha_l$  and  $\alpha_f$ , and upper terms  $(\alpha_u, \alpha'_u, \alpha''_u, \dots)$ . The illumination in the continuum can excite a virtual state between two contiguous configurations  $\alpha_u$  and  $\alpha'_u$ , inducing coherence effects between them.

hand, Rayleigh scattering in stellar atmospheres is dominated by contributions in the UV, particularly in the wings of H I  $\text{Ly}_\alpha$  around 121 nm, with the additional coherent contribution of the entire Lyman series (e.g., Stenflo 2005). Hence the importance for developing numerical tools that are adequate for the modeling of these spectral series.

Recently, several instruments for detecting the polarization of the solar spectrum in the UV have been developed or deployed. The Chromospheric Lyman-Alpha Spectro Polarimeter (CLASP; Kano et al. 2012) rocket experiment successfully measured the scattering polarization in H I  $\text{Ly}_\alpha$  and its variation along the solar radius (Kano et al. 2017). The results of this experiment confirmed important predictions from theoretical modeling of the Hanle effect in this line, but also opened new questions about the structure and magnetic topology of the upper solar chromosphere (Kano et al. 2017). Motivated by the CLASP success, and by ongoing efforts in the modeling of the Mg II h–k doublet in the solar transition region spectrum at 280 nm (Belluzzi & Trujillo Bueno 2012; Alsina Ballester, Belluzzi, & Trujillo Bueno 2016; del Pino Alemán, Casini, & Manso Sainz 2016), the CLASP-2 mission (Narukage et al. 2016) was proposed in order to measure the polarization produced by the joint action of scattering processes and the Hanle and Zeeman effects in these lines.

Other spectral structures of the solar UV spectrum offer additional insights in the energetics of the solar chromosphere and transition region, such as the Fe II UV multiplets between 230 and 260 nm (Anderson & Athay 1989; Judge, Jordan, & Feldman 1992). These transitions originate

from significantly more complex atomic structures than H I  $\text{Ly}_\alpha$  and Mg II h–k, and the modeling of the expected polarization signatures from these multiplets poses new challenges. One of them is to understand the physics of how the Fe II multiplets encompassed in this spectral region interact with each other to shape the overall spectral profile of the scattering polarization.

In this work, we rely on a recently proposed theoretical framework for the description of partially coherent scattering of polarized radiation (Casini et al. 2014; Casini & Manso Sainz 2016a), and extend it to the treatment of spectral series. In Section 2 we develop the extension of this formalism, and in Section 3 we apply our results to the modeling of the Fe II UV multiplets 1–3 (following the classification of Moore 1952). In the conclusive section, we discuss our findings, and provide a general physical explanation for the results, with a demonstration fully presented in the Appendix.

## 2. Radiation scattering in the multiple- $\Lambda$ atom

We recall the expression of the polarized emissivity for a  $\Lambda$ -type atom, taking into account partially coherent scattering (Casini & Manso Sainz 2016a),

$$\begin{aligned} \varepsilon_i^{(2)}(\omega_{k'}, \hat{\mathbf{k}}') &= \frac{4}{3} \frac{e_0^4}{\hbar^2 c^4} \mathcal{N} \omega_{k'}^4 \sum_{ll'} \rho_{ll'} \sum_{uu'f} \sum_{qq'} \sum_{pp'} (-1)^{q'+p'} (r_q)_{ul} (r_{q'})_{u'l'}^* (r_p)_{u'f} (r_{p'})_{uf}^* \\ &\times \sum_{KQ} \sum_{K'Q'} \sqrt{(2K+1)(2K'+1)} \begin{pmatrix} 1 & 1 & K \\ -q & q' & -Q \end{pmatrix} \begin{pmatrix} 1 & 1 & K' \\ -p & p' & -Q' \end{pmatrix} T_{Q'}^{K'}(i, \hat{\mathbf{k}}') \\ &\times \int_0^\infty d\omega_k \left( \Psi_{u'l',ful}^{-k,+k'-k} + \bar{\Psi}_{ul,fu'l'}^{-k,+k'-k} \right) J_Q^K(\omega_k), \quad (i = 0, 1, 2, 3) \end{aligned} \quad (1)$$

where  $i = 0, 1, 2, 3$  indicates the four Stokes parameters ( $I, Q, U, V$ ). The profiles  $\Psi$  describe the frequency redistribution of the incident radiation in the atomic rest of frame, and were defined by Casini et al. (2014). The transformation of the coherent emissivity (1) to the observer’s frame of reference is easily accomplished via the formal substitution

$$\Psi_{u'l',ful}^{-k,+k'-k} + \bar{\Psi}_{ul,fu'l'}^{-k,+k'-k} \rightarrow i(\Omega_{u'}^* - \Omega_u)^{-1} R(\Omega_u, \Omega_{u'}; \Omega_l, \Omega_{l'}, \Omega_f; \omega_k, \omega_{k'}, \Theta), \quad (2)$$

where  $R$  is the appropriate redistribution function in the “laboratory” frame of rest for the problem at hand,  $\Theta$  being the angle between the directions of the incident and emergent photons, and  $\Omega_a = \omega_a - i\epsilon_a$  the complex frequency of the atomic state  $a$  with level width  $\epsilon_a$ . For the examples illustrated in Section 3, we employed the laboratory frame redistribution function for the three-term atom of the  $\Lambda$  type (cf. Casini & Manso Sainz 2016b, and Figure 1). For the definition of all the other physical quantities in equation (1), the reader should refer to the paper of Casini et al. (2014).

In this section we extend equation (1) to the model of a multiple- $\Lambda$  atom (Figure 1) in the presence of a magnetic field. For simplicity, we derive the formalism for an atom without hyperfine structure, but the extension of the results to account for hyperfine structure is straightforward (Casini et al. 2014; Casini & Manso Sainz 2016a).

We indicate with  $\alpha_l$  and  $\alpha_f$  the electronic configurations of the initial and final terms of the  $\Lambda$  transition, and with  $(\alpha_u, \alpha'_u, \alpha''_u, \dots)$  the set of intermediate upper terms (Figure 1). We further assume the direction of the magnetic field as the quantization axis ( $z$ -axis). Then the atomic states involved in equation (1) are of the form

$$\begin{aligned} l &\equiv (\alpha_l \mu_l M_l) , & l' &\equiv (\alpha_l \mu'_l M'_l) , \\ u &\equiv (\alpha_u \mu_u M_u) , & u' &\equiv (\alpha'_u \mu'_u M'_u) , \\ f &\equiv (\alpha_f \mu_f M_f) , \end{aligned} \quad (3)$$

where  $M$  is the projection of the total angular momentum  $\mathbf{J} = \mathbf{L} + \mathbf{S}$  on the  $z$ -axis. The index  $\mu$  spans the eigenspace of the atomic Hamiltonian associated with a given value of  $M$  and term configuration  $\alpha$ . Hence, we assume a magnetic field regime such that configuration mixing induced by the magnetic Hamiltonian is negligible (see, e.g., Casini & Landi Degl’Innocenti 1993, Table 2, for an estimate of such condition in the case of the hydrogen atom). We then can write

$$|\alpha \mu M\rangle = \sum_J C_\mu^J(\alpha M) |\alpha J M\rangle ,$$

where the (real) projection coefficients  $C_\mu^J$  of the eigenstate  $|\alpha \mu M\rangle$  on the basis of the zero-field atomic states  $|\alpha J M\rangle$  satisfy the orthogonality conditions

$$\sum_J C_\mu^J(\alpha M) C_{\mu'}^J(\alpha M) = \delta_{\mu\mu'} , \quad \sum_\mu C_\mu^J(\alpha M) C_\mu^{J'}(\alpha M) = \delta_{JJ'} . \quad (4)$$

The density matrix element for the lower state,  $\rho_{ll'}$ , can be written in terms of the irreducible spherical tensor components of the statistical operator,

$$\begin{aligned} \rho_{ll'} &\equiv \langle \alpha_l \mu_l M_l | \rho | \alpha_l \mu'_l M'_l \rangle \\ &= \sum_{J_l} \sum_{J'_l} C_{\mu_l}^{J_l}(\alpha_l M_l) C_{\mu'_l}^{J'_l}(\alpha_l M'_l) \sum_{K_l Q_l} (-1)^{J_l - M_l} \sqrt{2K_l + 1} \begin{pmatrix} J_l & J'_l & K_l \\ M_l & -M'_l & -Q_l \end{pmatrix} \alpha_l \rho_{Q_l}^{K_l}(J_l, J'_l) , \end{aligned} \quad (5)$$

while use of the Wigner-Eckart theorem and its corollaries (e.g., Brink & Satchler 1993) gives the following expression for the dipole matrix element,

$$\begin{aligned} (r_q)_{ab} &\equiv \langle \alpha_a \mu_a M_a | r_q | \alpha_b \mu_b M_b \rangle \\ &= \sum_{J_a J_b} C_{\mu_a}^{J_a}(\alpha_a M_a) C_{\mu_b}^{J_b}(\alpha_b M_b) (-1)^{J_a - M_a} \sqrt{2J_a + 1} \begin{pmatrix} J_a & J_b & 1 \\ -M_a & M_b & q \end{pmatrix} \langle \alpha_a J_a || \mathbf{r} || \alpha_b J_b \rangle . \end{aligned} \quad (6)$$

To further proceed, we will assume that the multiple- $\Lambda$  atomic model is adequately described within the  $LS$ -coupling scheme, so that  $\alpha \equiv (\beta LS)$ , where  $\beta$  identifies the electronic configuration of a particular  $LS$  term of the atom. We then can write, additionally,

$$\begin{aligned} \langle \alpha_a J_a || \mathbf{r} || \alpha_b J_b \rangle &\equiv \langle \beta_a L_a S J_a || \mathbf{r} || \beta_b L_b S J_b \rangle . \\ &= (-1)^{1+L_a+S+J_b} \sqrt{(2L_a+1)(2J_b+1)} \begin{Bmatrix} J_a & J_b & 1 \\ L_b & L_a & S \end{Bmatrix} \mathbf{r}_{ab} , \end{aligned} \quad (7)$$

where we introduced the (generally complex) reduced matrix elements of the dipole operator between orbital configurations

$$\mathbf{r}_{ab} = \langle \beta_a L_a || \mathbf{r} || \beta_b L_b \rangle. \quad (8)$$

Using equations (5) through (8), equation (1) finally becomes

$$\begin{aligned} \varepsilon_i^{(2)}(\omega_{k'}, \hat{\mathbf{k}}') &= \frac{4}{3} \frac{e_0^4}{\hbar^2 c^4} \mathcal{N} \omega_{k'}^4 \Pi_{L_l L_f} \sum_{\beta_u L_u} \sum_{\beta'_u L'_u} (\mathbf{r}_{ul} \mathbf{r}_{uf}^*) (\mathbf{r}_{u'l}^* \mathbf{r}_{u'f}) \\ &\times \sum_{J_u J'_u J''_u J'''_u} \sum_{J_l J'_l J''_l J'''_l} \Pi_{J_u J'_u J''_u J'''_u} \Pi_{J_l J'_l J''_l J'''_l} \begin{Bmatrix} J_u & J_l & 1 \\ L_l & L_u & S \end{Bmatrix} \begin{Bmatrix} J'_u & J'_l & 1 \\ L_l & L'_u & S \end{Bmatrix} \begin{Bmatrix} J''_u & J_f & 1 \\ L_l & L_u & S \end{Bmatrix} \begin{Bmatrix} J'''_u & J'_f & 1 \\ L_l & L'_u & S \end{Bmatrix} \\ &\times \sum_{\mu_u M_u} \sum_{\mu'_u M'_u} \sum_{\mu_f M_f} C_{\mu_u}^{J_u}(M_u) C_{\mu'_u}^{J'_u}(M_u) C_{\mu'_u}^{J'_u}(M'_u) C_{\mu'_u}^{J''_u}(M'_u) C_{\mu_f}^{J_f}(M_f) C_{\mu_f}^{J'_f}(M_f) \\ &\times \sum_{\bar{J}_l \bar{J}'_l} \sum_{\mu_l M_l} \sum_{\mu'_l M'_l} C_{\mu_l}^{J_l}(M_l) C_{\mu_l}^{\bar{J}_l}(M_l) C_{\mu'_l}^{J'_l}(M'_l) C_{\mu'_l}^{\bar{J}'_l}(M'_l) \\ &\times \sum_{KQ} \sum_{K'Q'} \sum_{K_l Q_l} \sum_{q q'} \sum_{p p'} (-1)^{\bar{J}_l - M_l + q' + p'} \begin{pmatrix} 1 & 1 & K \\ -q & q' & -Q \end{pmatrix} \begin{pmatrix} 1 & 1 & K' \\ -p & p' & -Q' \end{pmatrix} \begin{pmatrix} \bar{J}_l & \bar{J}'_l & K_l \\ M_l & -M'_l & -Q_l \end{pmatrix} \\ &\times \begin{pmatrix} J_u & J_l & 1 \\ -M_u & M_l & q \end{pmatrix} \begin{pmatrix} J'_u & J'_l & 1 \\ -M'_u & M'_l & q' \end{pmatrix} \begin{pmatrix} J''_u & J_f & 1 \\ -M'_u & M_f & p \end{pmatrix} \begin{pmatrix} J''_u & J_f & 1 \\ -M_u & M_f & p' \end{pmatrix} \\ &\times \Pi_{KK'K_l} T_{Q'}^{K'}(i, \hat{\mathbf{k}}') \rho_{Q_l}^{K_l}(\bar{J}_l, \bar{J}'_l) \\ &\times \int_0^\infty d\omega_k \left( \Psi_{u'l', ful}^{-k, +k' - k} + \bar{\Psi}_{ul, fu'l'}^{-k, +k' - k} \right) J_Q^K(\omega_k), \quad (i = 0, 1, 2, 3) \end{aligned} \quad (9)$$

where for simplicity of notation we omitted the term information from the density matrix element and from the argument of the projection coefficients  $C_\mu^J$ , and also adopted the shorthand notation

$$\Pi_{ab...} \equiv \sqrt{(2a+1)(2b+1)\cdots}. \quad (10)$$

The reduced matrix elements  $\mathbf{r}_{ab}$  must be evaluated for each atomic species. In the case of complex atoms, this often requires a numerical modeling of the atomic structure (e.g., Hartree-Fock, Dirac-Hartree-Fock, etc.) in order to determine the atomic state wavefunctions. However, in the case of hydrogenic atoms, those matrix elements are purely real, and can be calculated with the aid of Gordon's formula (Bethe & Salpeter 1957, see also Casini & Landi Degl'Innocenti 1993). This allows, for example, to use the emissivity (9) to model the H I Lyman+Balmer contribution to the polarization of the solar continuum.

In this paper, instead, we focus on spectral series with a common lower term, i.e.,  $\alpha_f = \alpha_l$ , so the product of four  $\mathbf{r}_{ab}$  elements in equation (9) reduces to the product  $|\mathbf{r}_{ul}|^2 |\mathbf{r}_{u'l}|^2$ . This can conveniently be expressed in terms of the Einstein  $B_{lu}$  coefficient for absorption from the lower to the upper term of the atom, since

$$B_{lu} = \frac{16\pi^3}{3} \frac{e_0^2}{\hbar^2 c} \frac{\Pi_{L_u}^2}{\Pi_{L_l}^2} |\mathbf{r}_{ul}|^2. \quad (11)$$

Substitution of this equation into Equation (9) leads to the appearance of a product  $B_{lu}B_{lu'}$ . On the other hand, it is customary to make the Einstein coefficient for spontaneous emission,

$$A_{ul} = \frac{4}{3} \frac{e_0^2}{\hbar c^3} \omega_{ul}^3 |\mathbf{r}_{ul}|^2, \quad (12)$$

also explicitly appear in the expression for the 2nd-order emissivity (e.g., Casini & Manso Sainz 2016a). This can be accomplished using the well-known relation

$$B_{lu} = 4\pi^3 \frac{c^2}{\hbar \omega_{ul}^3} \frac{\Pi_{Lu}^2}{\Pi_{Ll}^2} A_{ul}. \quad (13)$$

It then becomes possible to rewrite the product  $B_{lu}B_{lu'}$  using one of the following equivalent forms (among others), which are symmetric with respect to the exchange of  $u$  and  $u'$ ,

$$\begin{aligned} B_{lu}B_{lu'} &= 2\pi^3 \frac{c^2}{\hbar} \frac{1}{\Pi_{Ll}^2} \left( \frac{\Pi_{Lu}^2}{\omega_{ul}^3} A_{ul} B_{lu'} + \frac{\Pi_{Lu'}^2}{\omega_{u'l}^3} A_{u'l} B_{lu} \right) \\ &= 4\pi^3 \frac{c^2}{\hbar} \frac{\Pi_{Lu} \Pi_{Lu'}}{\Pi_{Ll}^2} \left( \frac{A_{ul} A_{u'l} B_{lu} B_{lu'}}{\omega_{ul}^3 \omega_{u'l}^3} \right)^{1/2}. \end{aligned} \quad (14)$$

Here we adopt the second form, through which the 2nd-order emissivity (9) becomes,

$$\begin{aligned} \varepsilon_i^{(2)}(\omega_{k'}, \hat{\mathbf{k}}') &= \frac{3}{16\pi^3} \mathcal{N} \hbar \omega_{k'}^4 \Pi_{Ll}^2 \sum_{\beta_u L_u} \sum_{\beta_u' L_u'} \Pi_{Lu} \Pi_{Lu'} \left( \frac{A_{ul} A_{u'l} B_{lu} B_{lu'}}{\omega_{ul}^3 \omega_{u'l}^3} \right)^{1/2} \\ &\times \sum_{J_u J_u' J_u'' J_u'''} \sum_{J_l J_l' J_l'' J_l'''} \Pi_{J_u J_u' J_u'' J_u'''} \Pi_{J_l J_l' J_l'' J_l'''} \begin{Bmatrix} J_u & J_l & 1 \\ L_l & L_u & S \end{Bmatrix} \begin{Bmatrix} J_u' & J_l' & 1 \\ L_l & L_u' & S \end{Bmatrix} \begin{Bmatrix} J_u'' & J_l'' & 1 \\ L_l & L_u & S \end{Bmatrix} \begin{Bmatrix} J_u''' & J_l''' & 1 \\ L_l & L_u' & S \end{Bmatrix} \\ &\times \sum_{\mu_u M_u} \sum_{\mu_u' M_u'} \sum_{\mu_l' M_l''} C_{\mu_u}^{J_u}(M_u) C_{\mu_u'}^{J_u'}(M_u) C_{\mu_l'}^{J_l'}(M_l') C_{\mu_l''}^{J_l''}(M_l') C_{\mu_l'''}^{J_l'''}(M_l'') C_{\mu_l''''}^{J_l''''}(M_l'') \\ &\times \sum_{\bar{J}_l \bar{J}_l'} \sum_{\mu_l M_l} \sum_{\mu_l' M_l'} C_{\mu_l}^{J_l}(M_l) C_{\mu_l'}^{\bar{J}_l}(M_l) C_{\mu_l''}^{J_l'}(M_l') C_{\mu_l'''}^{\bar{J}_l'}(M_l') \\ &\times \sum_{KQ} \sum_{K'Q'} \sum_{K_l Q_l} \sum_{q q'} \sum_{p p'} (-1)^{\bar{J}_l - M_l + q' + p'} \begin{pmatrix} 1 & 1 & K \\ -q & q' & -Q \end{pmatrix} \begin{pmatrix} 1 & 1 & K' \\ -p & p' & -Q' \end{pmatrix} \begin{pmatrix} \bar{J}_l & \bar{J}_l' & K_l \\ M_l & -M_l' & -Q_l \end{pmatrix} \\ &\times \begin{pmatrix} J_u & J_l & 1 \\ -M_u & M_l & q \end{pmatrix} \begin{pmatrix} J_u' & J_l' & 1 \\ -M_u' & M_l' & q' \end{pmatrix} \begin{pmatrix} J_u'' & J_l'' & 1 \\ -M_u' & M_l'' & p \end{pmatrix} \begin{pmatrix} J_u''' & J_l''' & 1 \\ -M_u & M_l'' & p' \end{pmatrix} \\ &\times \Pi_{KK'K_l} T_{Q'Q}^{K'}(i, \hat{\mathbf{k}}') \rho_{Q_l}^{K_l}(\bar{J}_l, \bar{J}_l') \\ &\times \int_0^\infty d\omega_k \left( \Psi_{u'l', l'' ul}^{-k, +k' -k} + \bar{\Psi}_{ul, l'' u' l'}^{-k, +k' -k} \right) J_Q^K(\omega_k). \quad (i = 0, 1, 2, 3) \end{aligned} \quad (15)$$

In the following section, we apply equation (15) to the modeling of the polarized emissivity of spectral series with a common lower term  $\beta_l L_l$ .

### 3. Scattering Polarization of the Fe II UV Multiplets

An excellent illustration of the effects of  $L$ -term interference on the scattering polarization in spectral series, predicted by the 2nd-order emissivity (15), is provided by the first three UV multiplets of Fe II (following the classification of Moore 1952), which are visible in the solar spectrum between 230 and 265 nm.

For our modeling, we assume that the atomic system is illuminated by a collimated beam of light (i.e., with maximum anisotropy) without spectral structure, and we compute the Stokes vector scattered at  $90^\circ$  from the incidence direction. For the sake of demonstration, we only show calculations in the non-magnetic case, assuming a collisionless plasma at a temperature of  $T = 5000$  K. Since we have developed our formalism under the assumption that the magnetic field strength is small enough not to induce configuration mixing in the atomic system, magnetic effects, when included, will manifest around the transition resonances. In particular, they will appear as polarization signatures of the Hanle effect in the transition cores, and of  $J$ - $J'$  interference within each multiplet in the near wings. Collective effects encompassing the entire spectral series may also arise because of the common lower term of the series, which can be polarized, and therefore subject to the Hanle effect. However, such effects will also only manifest around the resonance frequency of the various atomic transitions in the series.

Recently, Alsina Ballester, Belluzzi, & Trujillo Bueno (2016) and del Pino Alemán, Casini, & Manso Sainz (2016; see also Manso Sainz, del Pino Alemán, & Casini 2017) have shown how PRD effects can combine with magneto-optical effects in an optically thick plasma to give rise to a significant  $Q \rightarrow U$  “rotation” of the scattering polarization in the near and far wings of deep resonance lines, even for magnetic strengths as small as a few gauss. Similar effects can be expected to manifest also for the model atom discussed in this paper. However, the necessary modeling effort involves the numerical solution of the full radiative transfer problem for polarized radiation in a realistic model atmosphere, which is beyond the scope of this paper.

The configuration of the UV multiplet series of Fe II presented here is well described within the  $LS$ -coupling scheme, with  $S = 5/2$ , and a common lower term with  $L_l = 2$ . Figure 2 shows the first UV multiplet at 261 nm, which corresponds to a  $\Delta L = L_u - L_l = 0$  transition, giving rise to 13 different  $\Delta J$  transition components. The top panel shows the intensity amplitude of the scattered radiation in logarithmic scale, with all 13 transition components resolved. The lower panel shows the corresponding fractional  $Q/I$  polarization. The gray profile in the lower panel models the case in which lower level polarization (l.l.p.) is neglected, whereas the black profile accounts for the presence of l.l.p. The two models are also drawn in the intensity plot, but they are essentially indistinguishable. The lower panel of Figure 2 reproduces Figure 10.27 of Landi Degl’Innocenti & Landolfi (2004), and is presented here mainly as a test of our model.

Figure 3 shows all three multiplets of the series, with multiplets 2 and 3 corresponding to the term transition  $\Delta L = +1$  (14 components) and  $\Delta L = -1$  (9 components), respectively. Multiplets 2 and 3 actually overlap in frequency, as shown in the intensity plot of Figure 3. These plots model the polarization of the scattered light over the three multiplets, assuming that the three corresponding term transitions are excited by the same collimated beam of unpolarized radiation,

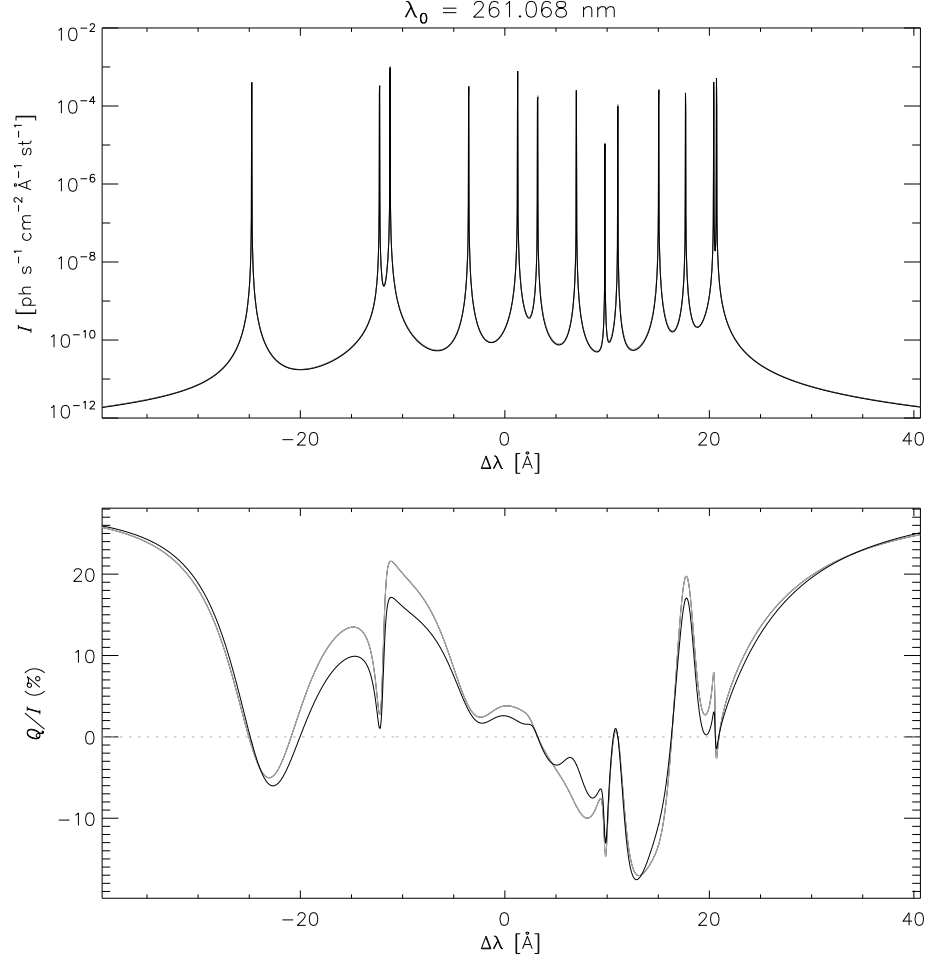


Fig. 2.— Intensity (top) and Stokes  $Q/I$  polarization (bottom) in  $90^\circ$  scattering and zero magnetic field, for the UV multiplet 1 of Fe II. Gray curve: neglecting lower-level atomic polarization (l.l.p); black curve: taking into account l.l.p. The bottom panel reproduces Figure 10.27 of Landi Degl’Innocenti & Landolfi (2004).

having a flat spectrum across the entire wavelength range of the series. The gray curve shows the emitted profile resulting from the incoherent addition of the individual contributions from the three multiplets. This is obtained by forcing the diagonality condition  $L'_u = L_u$  in the 2nd-order emissivity (15). The black profile instead takes into account the quantum interference among the three upper terms of the series. In both models, the effects of atomic polarization in the ground term are also fully accounted for. We note the striking difference in the behavior of the polarization, both in the far wings and around the center of gravity of the spectral group, when upper-term interference is properly taken into account.



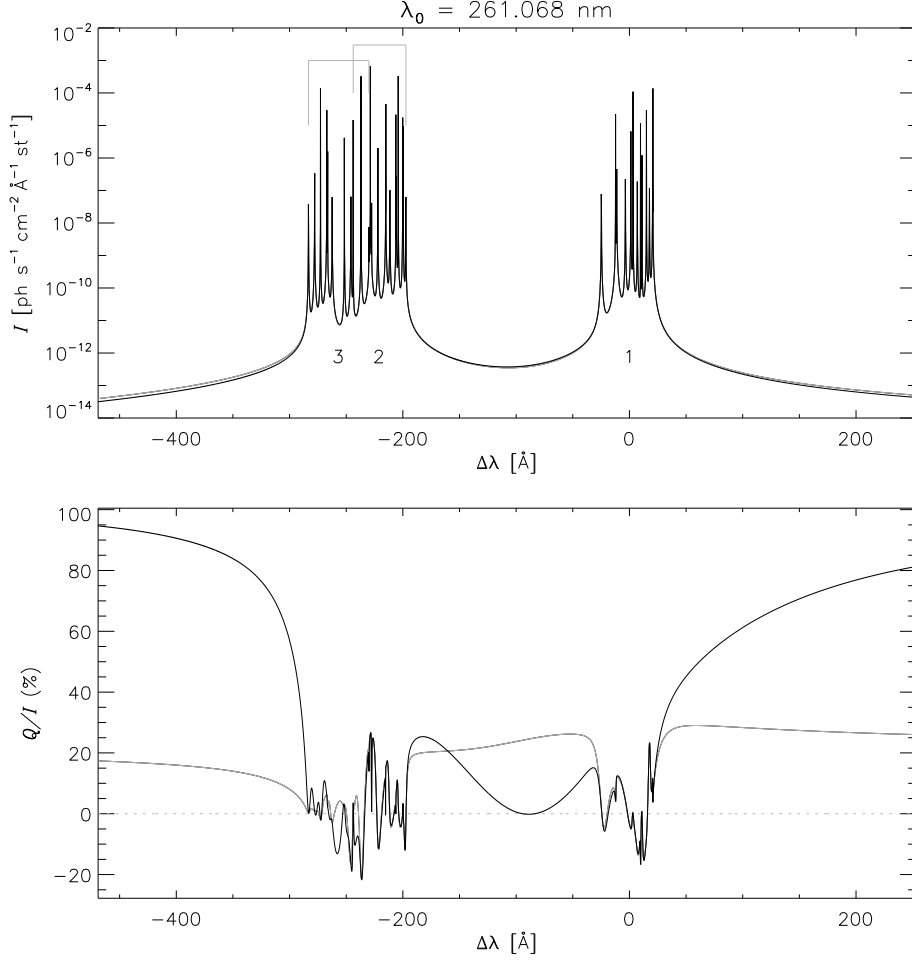


Fig. 3.— Intensity (top) and Stokes  $Q/I$  polarization (bottom) in  $90^\circ$  scattering and zero magnetic field, for the set of UV multiplets 1,2, and 3 ( $\Delta L = L_u - L_l = 0, +1, -1$ , respectively) of Fe II. We note that the component structures of multiplets 2 and 3 overlap, as indicated by the bounding boxes drawn at the top. Gray curve: neglecting upper  $L$ -term interference; black curve: taking into account upper  $L$ -term interference. We note the important depolarization effects around the center of gravity of the multiplet series, which are caused by the upper-term interference associated with the non-diagonal terms of the atomic density matrix. We also note the role of upper-term interference in causing the scattering polarization in the far wings of the spectral series to approach the upper limit of 100%.

#### 4. Discussion and Conclusions

The most notable feature of the modeled example of Fe II is the behavior of the  $Q/I$  polarization in the far wings of the series in the presence of  $L$ -term interference. When moving toward the neighboring continuum, this polarization approaches the theoretical limit of 100% expected for Rayleigh scattering—for the particular scattering model considered here, where the atom is irradi-

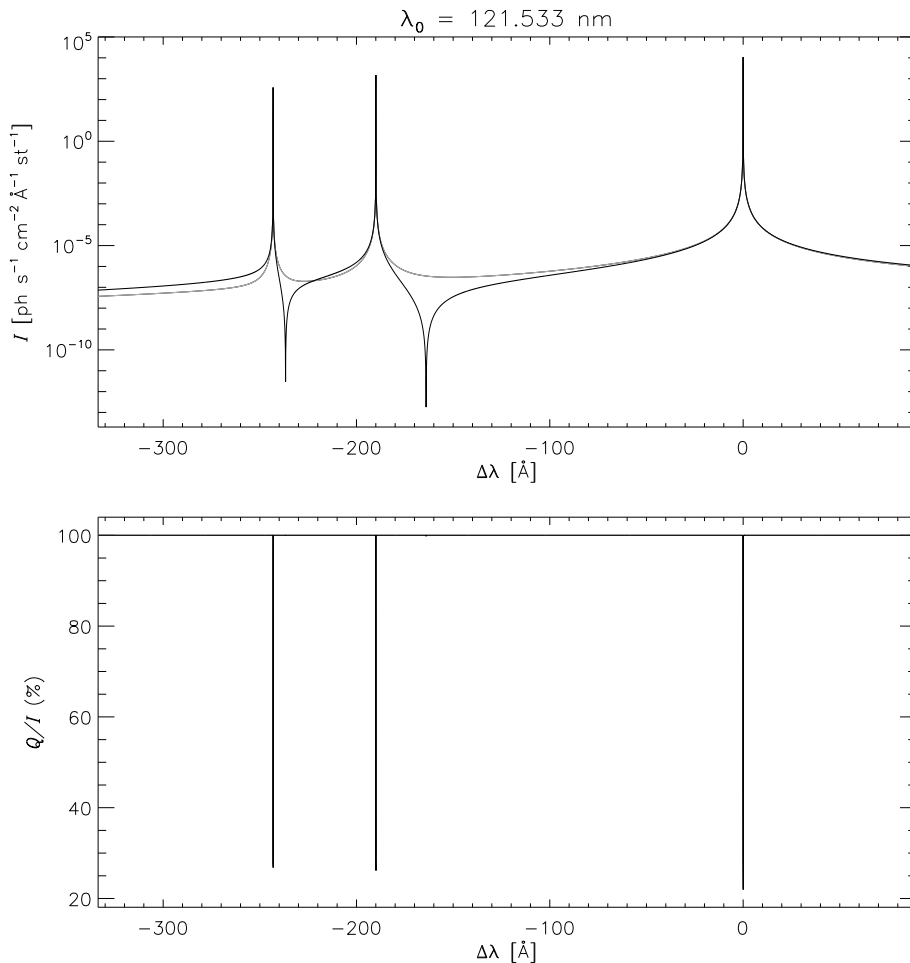


Fig. 4.— The first three lines of the H I Lyman series.

ated by a perfectly collimated beam of unpolarized light. This is a manifestation of the so-called *principle of spectroscopic stability* (e.g., Landi Degl’Innocenti & Landolfi 2004), according to which a complex system of atomic transitions between two fine-structured atomic terms must behave as a single transition between two simple terms with all the fine-structure details removed, in the experimental limit in which fine structure becomes unimportant. This is the case of the asymptotic behavior of the radiation scattered by a multiplet at a distance from its center of gravity much larger than the frequency span of its fine structure. In order to satisfy this principle, the system of atomic transitions must be “complete”, in the sense that the considered set of fine-structure components must satisfy some kind of sum rule, once the spectral details are ignored. Closure of this sum rule requires that all possible interference terms between different levels be taken into account, a condition that is evidently satisfied by equation (9).

In the appendix, we provide a formal derivation of the asymptotic behavior of the Stokes profiles, in the particular case of an unpolarized lower term, and determine the conditions under

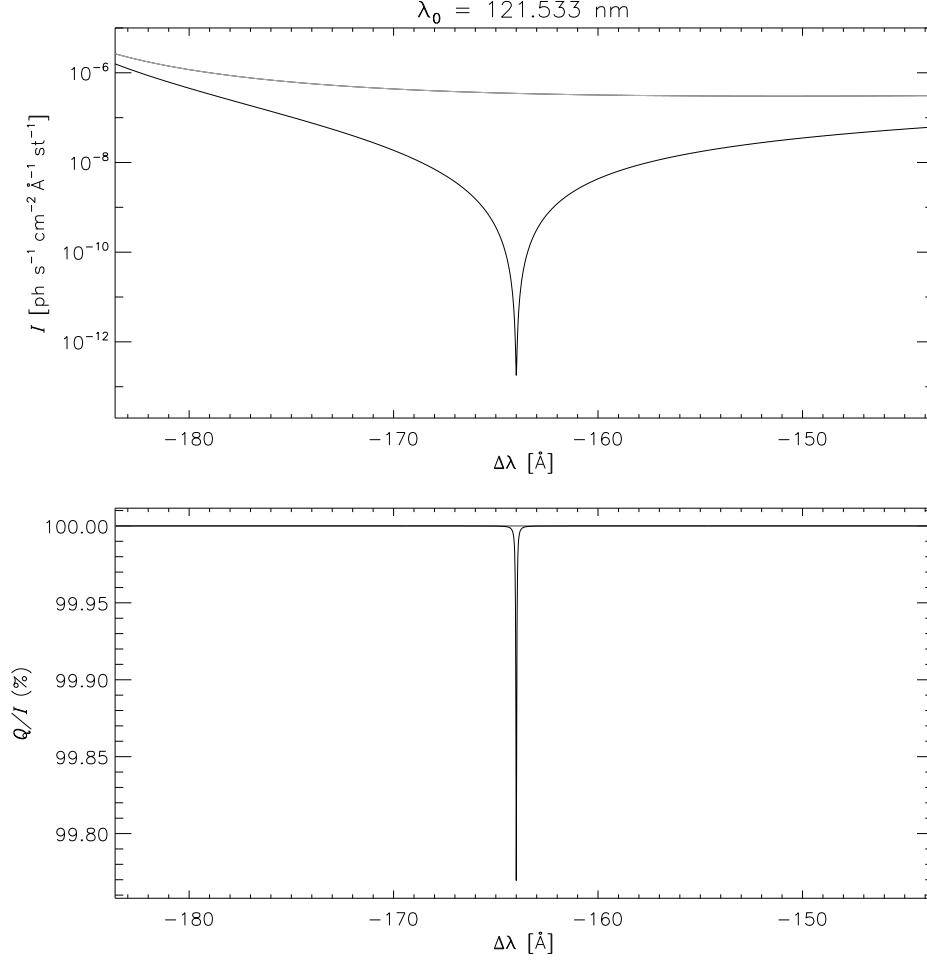


Fig. 5.— Spectral detail of the intensity dip structure in the red wing of H I  $\text{Ly}\beta$ .

which the theoretical limit of 100% polarization can be attained. We find that a necessary closure condition is that  $\Delta L$  attain all possible values allowed by the electric-dipole selection rule. When  $L_l \neq 0$ , these are obviously  $\Delta L = 0, \pm 1$ , otherwise we only have  $\Delta L = 1$ .

This last condition is verified in the case of the H I Lyman series, for *each* individual transition in the series. This is clearly illustrated by Figure 4, where the first three Lyman transitions of H I are shown, both neglecting (gray curve) and taking into account (black curve)  $L$ -term interference. In both cases, the  $Q/I$  polarization in the continuum between the lines attains the theoretical maximum of 100%. The intensity profile accounting for the effects of  $L$ -term interference agrees qualitatively with the results of Stenflo (2005). Most notably, the model that takes into account the  $L$ -term interference predicts the formation of intensity “dips” between lines of the series. Figure 5 shows the spectral details around the intensity dip in the right wing of  $\text{Ly}\beta$ , from which we see that these dips have a small depolarizing effect on the continuum. For the modeling of Figures 4 and 5 we adopted the same model of collisionless plasma as in Section 3.

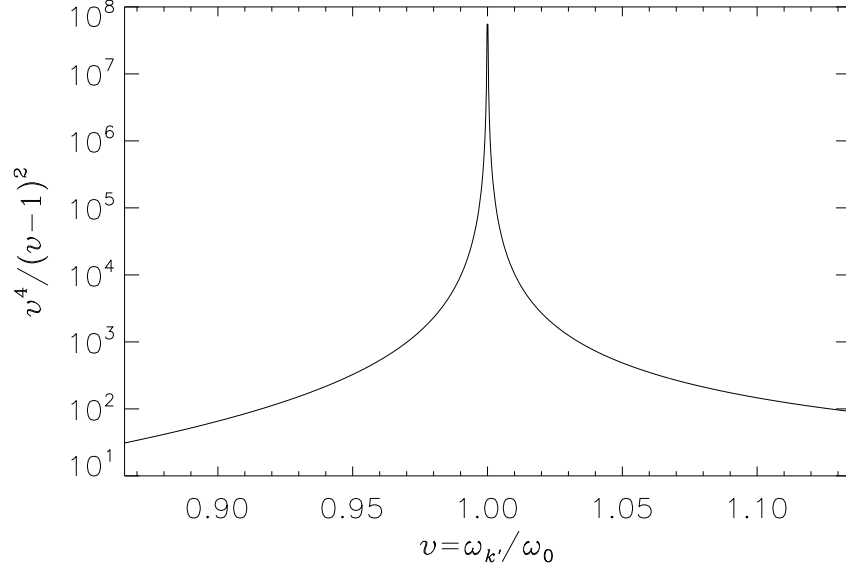


Fig. 6.— Plot showing the asymptotic behavior of the scattering profile  $\psi(v) = v^4/(v-1)^2$ , where  $v = \omega_{k'}/\omega_0$ . The adopted frequency range is comparable to the one adopted for Figure 3.

To conclude this section, we note that the presence of the lower-term density matrix  $\rho_{Q_l}^{K_l}(\bar{J}_l, \bar{J}_l')$  in the emissivity (15) requires the numerical solution of the (first order) statistical equilibrium (SE) problem for the polarized atom. In theory, in order for the model to be fully self-consistent, the SE problem should account for the same quantum interference effects among the upper terms of the spectral series that are included in the newly generalized form (15) of the 2nd-order emissivity.

For the numerical applications considered in this work, we did not generalize the SE problem in that sense. However, this does not affect the main results of this work, as the observed qualitative behavior of the polarization of a spectral series is reproduced even in the case of a naturally populated lower term (see Appendix).

We dedicate this work to the memory of our teacher, colleague, and friend Egidio Landi Degl’Innocenti (1945–2017). He “showed us the way”. We thank P. Judge (HAO) and J. Trujillo Bueno (IAC, HAO) for helpful discussion and comments on the manuscript.

### A. Asymptotic Limit of Scattering Polarization

We consider the 2nd-order emissivity (15) assuming that the lower term of the atomic system is unpolarized, with total population  $p_l$ , so that

$$\rho_{Q_l}^{K_l}(\bar{J}_l, \bar{J}_l') = \delta_{K_l 0} \delta_{Q_l 0} \delta_{\bar{J}_l \bar{J}_l'} \rho_0^0(\bar{J}_l), \quad p_l = \sum_{\bar{J}_l} \Pi_{\bar{J}_l} \rho_0^0(\bar{J}_l). \quad (\text{A1})$$

We look at the asymptotic behavior of the scattered Stokes profiles, i.e., at a frequency  $\omega_{k'}$  such that the following inequalities are both satisfied

$$|\omega_{k'} - \omega_0| \gg |\omega_{uu'}| \gtrsim \epsilon_{uu'} , \quad |\omega_{k'} - \omega_0| \gg |\omega_{ll'}| , \quad (\text{A2})$$

where we indicated with  $\omega_0$  the center of gravity of the system of transitions.

In the collisionless case, and under the usual assumption of a highly diluted radiation field,  $\epsilon_{l,l',l''} \rightarrow 0$  because of the implied infinite radiative lifetime of the lower levels. Under these assumptions, and in the asymptotic limit defined by the conditions (A2), the redistribution function behaves like

$$\Psi_{u'l',l''ul}^{-k,+k'-k} + \bar{\Psi}_{ul,l''u'l'}^{-k,+k'-k} \sim 2\pi \frac{\delta(\omega_{k'} - \omega_k)}{(\omega_{k'} - \omega_0)^2} . \quad (\text{A3})$$

(In order to see this one must consider the redistribution function (13) of Casini et al. (2014), noting that the conditions (A2) make the second term of that expression to vanish *at least* as  $(\omega_{k'} - \omega_0)^{-1}$ , whereas the  $\zeta$  functions in the first term force  $\omega_k$  to also be in the same asymptotic regime as  $\omega_{k'}$ . This finally leads to the asymptotic limit (A3).)

Then, equation (15) becomes, after using the orthogonality properties (4) and the integral norm of the redistribution function (cf. Casini et al. 2014, equation (15)),

$$\begin{aligned} \varepsilon_i^{(2)}(\omega_{k'}, \hat{\mathbf{k}}') &\sim \frac{3}{8\pi^2} \mathcal{N} \hbar \frac{\omega_{k'}^4}{(\omega_{k'} - \omega_0)^2} \Pi_{L_l}^2 \sum_{\beta_u L_u} \sum_{\beta'_u L'_u} \Pi_{L_u L'_u} \left( \frac{A_{ul} A_{u'l} B_{lu} B_{lu'}}{\omega_{ul}^3 \omega_{u'l}^3} \right)^{1/2} \\ &\times \sum_{J_u J'_u} \sum_{J_l J'_l} \Pi_{J_u J'_u J'_l}^2 \Pi_{J_l} \rho_0^0(J_l) \begin{Bmatrix} J_u & J_l & 1 \\ L_l & L_u & S \end{Bmatrix} \begin{Bmatrix} J'_u & J_l & 1 \\ L_l & L'_u & S \end{Bmatrix} \begin{Bmatrix} J_u & J'_l & 1 \\ L_l & L_u & S \end{Bmatrix} \begin{Bmatrix} J'_u & J'_l & 1 \\ L_l & L'_u & S \end{Bmatrix} \\ &\times \sum_{KQ} \sum_{K'Q'} \Pi_{KK'} J_Q^K(\omega_{k'}) T_{Q'}^{K'}(i, \hat{\mathbf{k}}') \sum_{M_u M'_u} \sum_{M_l M'_l} \sum_{qq'} \sum_{pp'} (-1)^{q'+p'} \begin{pmatrix} 1 & 1 & K \\ -q & q' & -Q \end{pmatrix} \begin{pmatrix} 1 & 1 & K' \\ -p & p' & -Q' \end{pmatrix} \\ &\times \begin{pmatrix} J_u & J_l & 1 \\ -M_u & M_l & q \end{pmatrix} \begin{pmatrix} J'_u & J_l & 1 \\ -M'_u & M_l & q' \end{pmatrix} \begin{pmatrix} J'_u & J'_l & 1 \\ -M'_u & M'_l & p \end{pmatrix} \begin{pmatrix} J_u & J'_l & 1 \\ -M_u & M'_l & p' \end{pmatrix} , \quad (i = 0, 1, 2, 3) \end{aligned} \quad (\text{A4})$$

We note that, despite the formal divergence of the ratio  $\omega_{k'}^4/(\omega_{k'} - \omega_0)^2$  at infinity, the resulting line profile remains well behaved even in the far wings of the spectral series (Figure 6).

In considering the asymptotic behavior of the emissivity (A4), the contraction of the full product of  $3j$ -symbols becomes possible, and is easily accomplished by summing over  $\{M_l, q, q'\}$ ,  $\{M'_l, p, p'\}$ , and  $\{M_u, M'_u\}$ , in that order. We then obtain

$$\begin{aligned} \varepsilon_i^{(2)}(\omega_{k'}, \hat{\mathbf{k}}') &\sim \frac{3}{8\pi^2} \mathcal{N} \hbar \frac{\omega_{k'}^4}{(\omega_{k'} - \omega_0)^2} \Pi_{L_l}^2 \sum_{\beta_u L_u} \sum_{\beta'_u L'_u} \Pi_{L_u L'_u} \left( \frac{A_{ul} A_{u'l} B_{lu} B_{lu'}}{\omega_{ul}^3 \omega_{u'l}^3} \right)^{1/2} \\ &\times \sum_{J_u J'_u} \sum_{J_l J'_l} (-1)^{J_l - J'_l} \Pi_{J_u J'_u J'_l}^2 \Pi_{J_l} \rho_0^0(J_l) \begin{Bmatrix} J_u & J_l & 1 \\ L_l & L_u & S \end{Bmatrix} \begin{Bmatrix} J'_u & J_l & 1 \\ L_l & L'_u & S \end{Bmatrix} \begin{Bmatrix} J_u & J'_l & 1 \\ L_l & L_u & S \end{Bmatrix} \begin{Bmatrix} J'_u & J'_l & 1 \\ L_l & L'_u & S \end{Bmatrix} \\ &\times \sum_{KQ} (-1)^Q \begin{Bmatrix} J_u & J'_u & K \\ 1 & 1 & J_l \end{Bmatrix} \begin{Bmatrix} J_u & J'_u & K \\ 1 & 1 & J'_l \end{Bmatrix} J_Q^K(\omega_{k'}) T_{-Q}^K(i, \hat{\mathbf{k}}') . \quad (i = 0, 1, 2, 3) \end{aligned} \quad (\text{A5})$$

The sums over  $J'_l$  and  $\{J_u, J'_u\}$  can also be performed, which leaves us simply with

$$\varepsilon_i^{(2)}(\omega_{k'}, \hat{\mathbf{k}}') \sim \frac{3}{8\pi^2} \mathcal{N} \hbar \frac{\omega_{k'}^4}{(\omega_{k'} - \omega_0)^2} p_l \sum_{KQ} (-1)^Q J_Q^K(\omega_{k'}) T_{-Q}^K(i, \hat{\mathbf{k}}') \quad (\text{A6})$$

$$\begin{aligned} & \times \sum_{\beta_u L_u} \sum_{\beta'_u L'_u} \Pi_{L_u L'_u} \left( \frac{A_{ul} A_{u'l} B_{lu} B_{lu'}}{\omega_{ul}^3 \omega_{u'l}^3} \right)^{1/2} \left\{ \begin{matrix} L_u & L'_u & K \\ 1 & 1 & L_l \end{matrix} \right\}^2 \\ & = \frac{3\pi}{2} \mathcal{N} c^2 \frac{\omega_{k'}^4}{(\omega_{k'} - \omega_0)^2} \frac{p_l}{\Pi_{L_l}^2} \sum_{KQ} (-1)^Q J_Q^K(\omega_{k'}) T_{-Q}^K(i, \hat{\mathbf{k}}') \\ & \times \sum_{\beta_u L_u} \sum_{\beta'_u L'_u} \Pi_{L_u L'_u}^2 \frac{A_{ul} A_{u'l}}{\omega_{ul}^3 \omega_{u'l}^3} \left\{ \begin{matrix} L_u & L'_u & K \\ 1 & 1 & L_l \end{matrix} \right\}^2, \quad (i = 0, 1, 2, 3) \end{aligned} \quad (\text{A7})$$

where we also used the definition of  $p_l$  in equation (A1), and in the second equivalence we used the relation (13) in order to express the summation over the atomic configurations of the excited states exclusively in terms of the Einstein  $A$ -coefficients. It is instructive to compare the form (A6) of the above expression with equation (10.148) of Landi Degl'Innocenti & Landolfi (2004), which describes the asymptotic behavior of the emissivity for a two-term atom, under the same hypotheses, and which can be used for modeling the case of Figure 2.

We now consider the following two conditions: 1) the ratio  $A_{ul}/\omega_{ul}^3$  is independent of  $u$ , and 2) the spectral series spans *all and only* the values of  $L_u$  that satisfy the triangular condition  $\Delta L = 0, \pm 1$ , i.e., the spectral series is *complete*. When  $L_l = 0$ , such as in the H I Lyman series, the triangular condition becomes simply  $L_u = 1$ , since  $0 \rightarrow 0$  transitions are strictly forbidden. Hence, *each* Lyman transition is *complete* in itself.

When both of the above conditions are met, either of the sums over  $L_u$  or  $L'_u$  in equation (A7) gives rise to the orthogonality (or closure) relation for the  $6j$  symbols (e.g., Brink & Satchler 1993), adding up to 1, whereas the remaining sum evaluates to  $3\Pi_l^2$ . In this case, the asymptotic  $Q/I$  polarization is simply given by the ratio

$$\frac{Q}{I} \sim \frac{\sum_{KQ} (-1)^Q J_Q^K(\omega_{k'}) T_{-Q}^K(1, \hat{\mathbf{k}}')}{\sum_{KQ} (-1)^Q J_Q^K(\omega_{k'}) T_{-Q}^K(0, \hat{\mathbf{k}}')}. \quad (\text{A8})$$

In particular, for  $90^\circ$  scattering by an atom illuminated with a collimated beam of unpolarized radiation, it can easily be shown that the above ratio equals 1.

In the case of the Fe II model of Figure 3, the invariance of  $A_{ul}/\omega_{ul}^3$  across the spectral series is only coarsely satisfied, since that quantity is in the ratios 48:42:36 for the UV multiplets 1, 2, and 3, respectively. Yet, even under such loose condition, the theoretical limit of  $Q/I$  as calculated through equation (A7) still lies above 99%.

The theoretical limit (A8) breaks down when the spectral series is not complete, in the sense specified above (e.g., in the case of the single multiplet of Figure 2), or when  $L$ -term quantum interference is neglected, which is the case shown by the gray curve in Figure 3. In fact, in such

case the double summation over electronic configurations in equation (A7) takes the diagonal form

$$\sum_{\beta_u L_u} \Pi_{L_u}^4 \left\{ \begin{matrix} L_u & L_u & K \\ 1 & 1 & L_l \end{matrix} \right\}^2,$$

which no longer corresponds to the closure relation for the  $6j$  symbols.

## REFERENCES

- Alsina Ballester, E., Belluzzi, L., & Trujillo Bueno, J. 2016, *ApJ*, 831, 15
- Anderson, L. S., & Athay, R. G. 1989, *ApJ*, 346, 1010
- Belluzzi, L. & Trujillo Bueno, J. 2012, *ApJ*, 750, 11
- Bethe, H. A., & Salpeter, E. E. 1957, *Quantum Mechanics of One- and Two-Electron Atoms* (New York: Academic Press)
- Brink, D. M., & Satchler, G. R. 1993, *Angular Momentum*, 3rd ed. (Oxford: Clarendon)
- Casini, R., & Landi Degl’Innocenti, E. 1993, *A&A*, 276, 289
- Casini, R., Landi Degl’Innocenti, M., Manso Sainz, R., Landi Degl’Innocenti, E., & Landolfi, M.. 2014, *ApJ*, 791, 94
- Casini, R., & Manso Sainz, R.. 2016, *ApJ*, 825, 135
- Casini, R., & Manso Sainz, R.. 2016, *ApJ*, 833, 197
- Ivanov, V. V. 1991, in *NATO ASIC Proc. 341: Stellar Atmospheres–Beyond Classical Models*, ed. L. Crivellari, I. Hubeny, & D. G. Hummer (Dordrecht: Kluwer), 81
- Judge, P. G., Jordan, C., & Feldman, U. 1992, *ApJ*, 384, 613
- Kano, R., Bando, T., Narukage, N., et al. 2012, *SPIE*, 8443, 4F
- Kano, R., Trujillo Bueno, J., Winebarger, A., et al. 2017, *ApJ*, 839, 10
- Malitson, H. H., Purcell, J. D., Tousey, R., & Moore, C. E. 1960, *ApJ*, 132, 746
- Manso Sainz, R., del Pino Alemán, T., & Casini, R. 2017, in *Solar Polarization Workshop 8, ASP Conf. Ser., Vol. XXX*, eds. L. Belluzzi, R. Casini, M. Romoli, J. Trujillo Bueno (San Francisco: ASP), YYY (arXiv:1710.04155)
- Moore, C. E. 1952, *Atomic Energy Levels*, Vol. II, National Bureau of Standards
- del Pino Alemán, T., Casini, R., & Manso Sainz, R. 2016, *ApJ*, 830, L24

- Landi Degl’Innocenti, E., & Landolfi, M. 2004, *Polarization in Spectral Lines* (Dordrecht: Springer)
- Narukage, N., McKenzie, D. E., Ishikawa, R., et al. 2016, *SPIE*, 9905, 08
- Stenflo, J. O. 2005, *A&A*, 4289, 713
- Stenflo, J. O. 2011, in *Solar Polarization Workshop 6*, ASP Conf. Ser., Vol. XXX, eds. J. R. Kuhn et al. (San Francisco: ASP), 3
- Stenflo, J. O. 2015, *SSRv*, doi:10.1007/s11214-015-0198-z
- Stenflo, J. O., & Keller, C. U. 1997, *A&A*, 321, 927
- Trujillo Bueno, J., Landi Degl’Innocenti, E., & Belluzzi, L. 2017, *SSRv*, doi:10.1007/s11214-016-0306-8